
Compositional Reinforcement Learning from Logical Specifications

Kishor Jothimurugan
University of Pennsylvania

Suguman Bansal
University of Pennsylvania

Osbert Bastani
University of Pennsylvania

Rajeev Alur
University of Pennsylvania

Abstract

We study the problem of learning control policies for complex tasks given by logical specifications. Recent approaches automatically generate a reward function from a given specification and use a suitable reinforcement learning algorithm to learn a policy that maximizes the expected reward. These approaches, however, scale poorly to complex tasks that require high-level planning. In this work, we develop a compositional learning approach, called D_IRL, that interleaves high-level planning and reinforcement learning. First, D_IRL encodes the specification as an abstract graph; intuitively, vertices and edges of the graph correspond to regions of the state space and simpler sub-tasks, respectively. Our approach then incorporates reinforcement learning to learn neural network policies for each edge (sub-task) within a Dijkstra-style planning algorithm to compute a high-level plan in the graph. An evaluation of the proposed approach on a set of challenging control benchmarks with continuous state and action spaces demonstrates that it outperforms state-of-the-art baselines.

1 Introduction

Reinforcement learning (RL) is a promising approach to automatically learning control policies for continuous control tasks—e.g., for challenging tasks such as walking [10] and grasping [6], control of multi-agent systems [27, 18], and control from visual inputs [24]. A key challenge facing RL is the difficulty in specifying the goal. Typically, RL algorithms require the user to provide a reward function that encodes the desired task. However, for complex, long-horizon tasks, providing a suitable reward function can be a daunting task, requiring the user to manually compose rewards for individual subtasks. Poor reward functions can make it hard for the RL algorithm to achieve the goal; e.g., it can result in reward hacking [3], where the agent learns to optimize rewards without achieving the goal.

Recent work has proposed a number of high-level languages for specifying RL tasks [5, 25, 20, 30, 16]. A key feature of these approaches is that they enable the user to specify tasks *compositionally*—i.e., the user can independently specify a set of short-term subgoals, and then ask the robot to perform a complex task that involves achieving some of these subgoals. Existing approaches for learning from high-level specifications typically generate a reward function, which is then used by an off-the-shelf RL algorithm to learn a policy. Recent works based on Reward Machines [16, 31] have proposed RL algorithms that exploit the structure of the specification to improve learning. However, these algorithms are based on model-free RL at both the high- and low-levels instead of model-based RL. Model-free RL has been shown to outperform model-based approaches on low-level control tasks [9]; however, at the high-level, it is unable to exploit the large amount of available structure. Thus, these approaches scale poorly to long horizon tasks involving complex decision making.

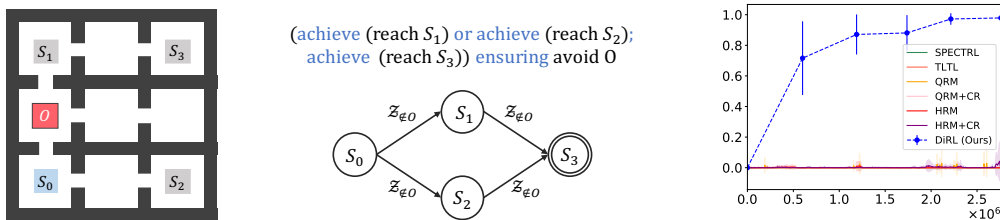


Figure 1: Left: The 9-rooms environment, with initial region S_0 in the bottom-left, an obstacle O in the middle-left, and three subgoal regions S_1, S_2, S_3 in the remaining corners. Middle top: A user-provided specification ϕ_{ex} . Middle bottom: The abstract graph \mathcal{G}_{ex} DfRL constructs for ϕ_{ex} . Right: Learning curves for our approach and some baselines; x -axis is number of steps and y -axis is probability of achieving ϕ_{ex} .

We propose DfRL, a novel compositional RL algorithm that leverages the structure in the specification to decompose the policy synthesis problem into a high-level planning problem and a set of low-level control problems. Then, it interleaves model-based high-level planning with model-free RL to compute a policy that tries to maximize the probability of satisfying the specification. In more detail, our algorithm begins by converting the user-provided specification into an abstract graph whose edges encode the subtasks, and whose vertices encode regions of the state space where each subtask is considered achieved. Then, it uses a Dijkstra-style forward graph search algorithm to compute a sequence of subtasks for achieving the specification, aiming to maximize the success probability. Rather than compute a policy to achieve each subtask beforehand, it constructs them on-the-fly for a subtask as soon as Dijkstra’s algorithm requires the cost of that subtask.

We empirically evaluate our approach on a “rooms environment” (with continuous state and action spaces), where a 2D agent must navigate a set of rooms to achieve the specification, as well as a challenging “fetch environment” where the goal is to use a robot arm to manipulate a block to achieve the specification. We demonstrate that DfRL significantly outperforms state-of-the-art deep RL algorithms for learning policies from specifications, such as SPECTRL, TLTL, QRM and HRM, as the complexity of the specification increases. In particular, by exploiting the structure of the specification to decouple high-level planning and low-level control, the sample complexity of DfRL scales roughly linearly in the size of the specification, whereas the baselines quickly degrade in performance. Our results demonstrate that DfRL is capable of learning to achieve complex tasks in challenging continuous control environments.

Motivating example. Consider an RL-agent in the environment of interconnected rooms in Figure 1. The agent is initially in the blue box, and their goal is to navigate to either the top-left room S_1 or the bottom-right room S_2 , followed by the top-right room S_3 , all the while avoiding the red block O . This goal is formally captured by the SPECTRL specification ϕ_{ex} (middle top). This specification is comprised of four simpler RL subtasks—namely, navigating between the corner rooms while avoiding the obstacle. Our approach, DfRL, leverages this structure to improve learning. First, based on the specification alone, it constructs the abstract graph \mathcal{G}_{ex} (see middle bottom) whose vertices represent the initial region and the three subgoal regions, and the edges correspond to subtasks (labeled with a safety constraint that must be satisfied).

However, \mathcal{G}_{ex} by itself is insufficient to determine the optimal path—e.g., it does not know that there is no path leading directly from S_2 to S_3 , which is a property of the environment. These differences can be represented as (*a priori* unknown) edge costs in \mathcal{G}_{ex} . At a high level, DfRL trains a policy π_e for each edge e in \mathcal{G}_{ex} , and sets the cost of e to be $c(e; \pi_e) = -\log P(e; \pi_e)$, where $P(e; \pi_e)$ is the probability that π_e succeeds in achieving e . For instance, for the edge $S_0 \rightarrow S_1$, π_e is trained to reach S_1 from a random state in S_0 while avoiding O . Then, a naive strategy for identifying the optimal path is to (i) train a policy π_e for each edge e , (ii) use it to estimate the edge cost $c(e; \pi_e)$, and (iii) run Dijkstra’s algorithm with these costs.

One challenge is that π_e depends on the initial states used in its training—e.g., training π_e for $e = S_1 \rightarrow S_3$ requires a distribution over S_1 . Using the wrong distribution can lead to poor performance due to distribution shift; furthermore, training a policy for all edges may unnecessarily waste effort training policies for unimportant edges. To address these challenges, DfRL interweaves training policies with the execution of Dijkstra’s algorithm, only training π_e once Dijkstra’s algorithm

requires the cost of edge e . This strategy enables D_IRL to scale to complex tasks; in our example, it quickly learns a policy that satisfies the specification with high probability. These design choices are validated empirically—as shown in Figure 1, D_IRL quickly learns to achieve the specification, whereas it is beyond the reach of existing approaches.

Related Work. There has been recent work on using specifications based on temporal logic for specifying RL tasks [2, 15, 26, 14, 35, 12, 34, 19]. These approaches typically generate a (usually sparse) reward function from a given specification which is then used by an off-the-shelf RL algorithm to learn a policy. In particular, Li et al. [25] propose a variant of Linear Temporal Logic (LTL) called TLTL to specify tasks for robots, and then derive shaped (continuous) rewards from specifications in this language. Jothimurugan et al. [20] propose a specification language called SPECTRL that allows users to encode complex tasks involving sequences, disjunctions, and conjunctions of subtasks, as well as specify safety properties; then, given a specification, they construct a finite state machine called a *task monitor* that is used to obtain shaped (continuous) rewards. Icarte et al. [16] propose an automaton based model called *reward machines* (RM) for high-level task specification and decomposition as well as an RL algorithm (QRM) that exploits this structure. In a later paper [31], they propose variants of QRM including an hierarchical RL algorithm (HRM) to learn policies for tasks specified using RMs. Camacho et al. [8] show that one can generate RMs from temporal specifications but RMs generated this way lead to sparse rewards. Kuo et al. [23] propose a compositional model for zero-shot execution of LTL formulas but training such a model requires a lot of samples even for relatively simpler environments. There has also been recent work on using temporal logic specifications for multi-agent RL [13, 29].

More broadly, there has been work on using *policy sketches* [5], which are sequences of subtasks designed to achieve the goal. They show that such approaches can speed up learning for long-horizon tasks. Sun et al. [30] show that providing semantics to the subtasks (e.g., encode rewards that describe when the subtask has been achieved) can further speed up learning. There has also been recent interest in combining high-level planning with reinforcement learning [1, 21]. These approaches all target MDPs with reward functions, whereas we target MDPs with logical task specifications. Furthermore, in our setting, the high-level structure is derived from the given specification, whereas in existing approaches it is manually provided. Finally, there has been recent work on applying formal reasoning for extracting interpretable policies [32, 33, 17] as well as for safe reinforcement learning [4, 22].

2 Problem Formulation

MDP. We consider a *Markov decision process* (MDP) $\mathcal{M} = (S, A, P, \eta)$ with continuous states $S \subseteq \mathbb{R}^n$, continuous actions $A \subseteq \mathbb{R}^m$, transitions $P(s, a, s') = p(s' | s, a) \in \mathbb{R}_{\geq 0}$ (i.e., the probability density of transitioning from state s to state s' upon taking action a), and initial states $\eta : S \rightarrow \mathbb{R}_{\geq 0}$ (i.e., $\eta(s)$ is the probability density of the initial state being s). A *trajectory* $\zeta \in \mathcal{Z}$ is either an infinite sequence $\zeta = s_0 \xrightarrow{a_0} s_1 \xrightarrow{a_1} \dots$ or a finite sequence $\zeta = s_0 \xrightarrow{a_0} \dots \xrightarrow{a_{t-1}} s_t$ where $s_i \in S$ and $a_i \in A$. A subtrajectory of ζ is a subsequence $\zeta_{\ell:k} = s_\ell \xrightarrow{a_\ell} \dots \xrightarrow{a_{k-1}} s_k$. We let \mathcal{Z}_f denote the set of finite trajectories. A (deterministic) *policy* $\pi : \mathcal{Z}_f \rightarrow A$ maps a finite trajectory to a fixed action. Given π , we can sample a trajectory by sampling an initial state $s_0 \sim \eta(\cdot)$, and then iteratively taking the action $a_i = \pi(\zeta_{0:i})$ and sampling a next state $s_{i+1} \sim p(\cdot | s_i, a_i)$.

Specification language. We consider the specification language SPECTRL for specifying reinforcement learning tasks [20]. A specification ϕ in this language is a logical formula over trajectories that indicates whether a given trajectory ζ successfully accomplishes the desired task. As described below, it can be interpreted as a function $\phi : \mathcal{Z} \rightarrow \mathbb{B}$, where $\mathbb{B} = \{\text{true}, \text{false}\}$.

Formally, a specification is defined over a set of *atomic predicates* \mathcal{P}_0 , where every $p \in \mathcal{P}_0$ is associated with a function $\llbracket p \rrbracket : S \rightarrow \mathbb{B}$; we say a state s *satisfies* p (denoted $s \models p$) if and only if $\llbracket p \rrbracket(s) = \text{true}$. For example, given a state $s \in S$, the atomic predicate $\llbracket \text{reach } s \rrbracket(s') = (\|s' - s\| < 1)$ indicates whether the system is in a state close to s with respect to the norm $\|\cdot\|$. The set of *predicates* \mathcal{P} consists of conjunctions and disjunctions of atomic predicates. The syntax of a predicate $b \in \mathcal{P}$ is given by the grammar $b ::= p \mid (b_1 \wedge b_2) \mid (b_1 \vee b_2)$, where $p \in \mathcal{P}_0$. Similar to atomic predicates, each predicate $b \in \mathcal{P}$ corresponds to a function $\llbracket b \rrbracket : S \rightarrow \mathbb{B}$ defined naturally over

Boolean logic. Finally, the syntax of SPECTRL specifications is given by ¹

$$\phi ::= \text{achieve } b \mid \phi_1 \text{ ensuring } b \mid \phi_1; \phi_2 \mid \phi_1 \text{ or } \phi_2,$$

where $b \in \mathcal{P}$. In this case, each specification ϕ corresponds to a function $\llbracket \phi \rrbracket : \mathcal{Z} \rightarrow \mathbb{B}$, and we say $\zeta \in \mathcal{Z}$ satisfies ϕ (denoted $\zeta \models \phi$) if and only if $\llbracket \phi \rrbracket(\zeta) = \text{true}$. Letting ζ be a finite trajectory of length t , this function is defined by

$$\begin{aligned} \zeta \models \text{achieve } b & && \text{if } \exists i \leq t, s_i \models b \\ \zeta \models \phi \text{ ensuring } b & && \text{if } \zeta \models \phi \text{ and } \forall i \leq t, s_i \models b \\ \zeta \models \phi_1; \phi_2 & && \text{if } \exists i < t, \zeta_{0:i} \models \phi_1 \text{ and } \zeta_{i+1:t} \models \phi_2 \\ \zeta \models \phi_1 \text{ or } \phi_2 & && \text{if } \zeta \models \phi_1 \text{ or } \zeta \models \phi_2. \end{aligned}$$

Intuitively, the first clause means that the trajectory should eventually reach a state that satisfies the predicate b . The second clause says that the trajectory should satisfy specification ϕ while always staying in states that satisfy b . The third clause says that the trajectory should sequentially satisfy ϕ_1 followed by ϕ_2 . The fourth clause means that the trajectory should satisfy either ϕ_1 or ϕ_2 . An infinite trajectory ζ satisfies ϕ if there is a t such that the prefix $\zeta_{0:t}$ satisfies ϕ .

Learning from Specifications. Given an MDP \mathcal{M} with unknown transitions and a specification ϕ , our goal is to compute a policy $\pi^* : \mathcal{Z}_f \rightarrow \mathcal{A}$ such that $\pi^* \in \arg \max_{\pi} \Pr_{\zeta \sim \mathcal{D}_{\pi}}[\zeta \models \phi]$, where \mathcal{D}_{π} is the distribution over infinite trajectories generated by π . In other words, we want to learn a policy π^* that maximizes the probability that a generated trajectory ζ satisfies the specification ϕ .

3 Abstract Reachability

In this section, we describe how to reduce the RL problem for a given MDP \mathcal{M} and specification ϕ to a reachability problem on a directed acyclic graph (DAG) \mathcal{G}_{ϕ} , augmented with information connecting its edges to subtrajectories in \mathcal{M} . In Section 4, we describe how to exploit the compositional structure of \mathcal{G}_{ϕ} to learn efficiently.

3.1 Abstract Reachability

We begin by defining the *abstract reachability* problem, and describe how to reduce the problem of learning from a SPECTRL specification to abstract reachability. At a high level, abstract reachability is defined as a graph reachability problem over a directed acyclic graph (DAG) whose vertices correspond to *subgoal regions*—a subgoal region $X \subseteq S$ is a subset of the state space S . As discussed below, in our reduction, these subgoal regions are derived from the given specification ϕ . The constructed graph structure also encodes the relationships between subgoal regions.

Definition 3.1. An *abstract graph* $\mathcal{G} = (U, E, u_0, F, \beta, \mathcal{Z}_{\text{safe}})$ is a directed cyclic graph (DAG) with vertices U , (directed) edges $E \subseteq U \times U$, initial vertex $u_0 \in U$, final vertices $F \subseteq U$, subgoal region map $\beta : U \rightarrow 2^S$ such that for each $u \in U$, $\beta(u)$ is a subgoal region,² and *safe trajectories* $\mathcal{Z}_{\text{safe}} = \bigcup_{e \in E} \mathcal{Z}_{\text{safe}}^e$, where $\mathcal{Z}_{\text{safe}}^e \subseteq \mathcal{Z}_f$ denotes the safe trajectories for edge $e \in E$.

Intuitively, (U, E) is a standard DAG, and u_0 and F define a graph reachability problem for (U, E) . Furthermore, β and $\mathcal{Z}_{\text{safe}}$ connect (U, E) back to the original MDP \mathcal{M} ; in particular, for an edge $e = u \rightarrow u'$, $\mathcal{Z}_{\text{safe}}^e$ is the set of trajectories in \mathcal{M} that can be used to transition from $\beta(u)$ to $\beta(u')$.

Definition 3.2. An infinite trajectory $\zeta = s_0 \xrightarrow{a_0} s_1 \xrightarrow{a_1} \dots$ in \mathcal{M} satisfies *abstract reachability* for \mathcal{G} (denoted $\zeta \models \mathcal{G}$) if there is a sequence of indices $0 = i_0 \leq i_1 < \dots < i_k$ and a path $\rho = u_0 \rightarrow u_1 \rightarrow \dots \rightarrow u_k$ in \mathcal{G} such that

- $u_k \in F$,
- for all $j \in \{0, \dots, k\}$, we have $s_{i_j} \in \beta(u_j)$, and
- for all $j < k$, letting $e_j = u_j \rightarrow u_{j+1}$, we have $\zeta_{i_j:i_{j+1}} \in \mathcal{Z}_{\text{safe}}^{e_j}$.

¹Here, *achieve* and *ensuring* correspond to the “eventually” and “always” operators in temporal logic.

²We do not require that the subgoal regions partition the state space or that they be non-overlapping.

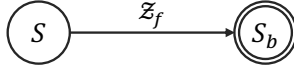


Figure 2: Abstract graph for achieve b .

The first two conditions state that the trajectory should visit a sequence of subgoal regions corresponding to a path from the initial vertex to some final vertex, and the last condition states that the trajectory should be composed of subtrajectories that are safe according to $\mathcal{Z}_{\text{safe}}$.

Definition 3.3. Given MDP \mathcal{M} with unknown transitions and abstract graph \mathcal{G} , the *abstract reachability problem* is to compute a policy $\tilde{\pi} : \mathcal{Z}_f \rightarrow A$ such that $\tilde{\pi} \in \arg \max_{\pi} \Pr_{\zeta \sim \mathcal{D}_{\pi}} [\zeta \models \mathcal{G}]$.

In other words, the goal is to find a policy for which the probability that a generated trajectory satisfies abstract reachability is maximized.

3.2 Reduction to Abstract Reachability

Next, we describe how to reduce the RL problem for a given MDP \mathcal{M} and a specification ϕ to an abstract reachability problem for \mathcal{M} by constructing an abstract graph \mathcal{G}_{ϕ} inductively from ϕ . We give a high-level description here, and provide details in Appendix A in the supplement.

First, for each predicate b , we define the corresponding subgoal region $S_b = \{s \in S \mid s \models b\}$ denoting the set of states at which b holds. Next, the abstract graph \mathcal{G}_{ϕ} for $\phi = \text{achieve } b$ is shown in Figure 2. All trajectories in \mathcal{Z}_f are considered safe for the edge $e = u_0 \rightarrow u_1$ and the only final vertex is u_1 with $\beta(u_1) = S_b$. The abstract graph for a specification of the form $\phi = \phi_1 \text{ ensuring } b$ is obtained by taking the graph \mathcal{G}_{ϕ_1} and replacing the set of safe trajectories $\mathcal{Z}_{\text{safe}}^e$, for each $e \in E$, with the set $\mathcal{Z}_{\text{safe}}^e \cap \mathcal{Z}_b$, where $\mathcal{Z}_b = \{\zeta \in \mathcal{Z}_f \mid \forall i. s_i \models b\}$ is the set of trajectories in which all states satisfy b . For the sequential specification $\phi = \phi_1; \phi_2$, we construct \mathcal{G}_{ϕ} by adding edges from every final vertex of \mathcal{G}_{ϕ_1} to every vertex of \mathcal{G}_{ϕ_2} that is a neighbor of its initial vertex. Finally, choice $\phi = \phi_1 \text{ or } \phi_2$ is handled by merging the initial vertices of the graphs corresponding to the two sub-specifications. Figure 1 shows an example abstract graph. The labels on the vertices are regions in the environment. All trajectories that avoid hitting the obstacle O are safe for all edges. We have the following key guarantee:

Theorem 3.4. *Given a SPECTRL specification ϕ , we can construct an abstract graph \mathcal{G}_{ϕ} such that, for every infinite trajectory $\zeta \in \mathcal{Z}$, we have $\zeta \models \phi$ if and only if $\zeta \models \mathcal{G}_{\phi}$. Furthermore, the number of vertices in \mathcal{G}_{ϕ} is $O(|\phi|)$ where $|\phi|$ is the size of the specification ϕ .*

We give a proof in Appendix A. As a consequence, we can solve the reinforcement learning problem for ϕ by solving the abstract reachability problem for \mathcal{G}_{ϕ} . As described below, we leverage the structure of \mathcal{G}_{ϕ} in conjunction with reinforcement learning to do so.

4 Compositional Reinforcement Learning

In this section, we propose a compositional approach for learning a policy to solve the abstract reachability problem for MDP \mathcal{M} (with unknown transition probabilities) and abstract graph \mathcal{G} .

4.1 Overview

At a high level, our algorithm proceeds in three steps:

- For each edge $e = u \rightarrow u'$ in \mathcal{G} , use RL to learn a neural network (NN) policy π_e to try and transition the system from any state $s \in \beta(u)$ to some state $s' \in \beta(u')$ in a safe way according to $\mathcal{Z}_{\text{safe}}^e$. Importantly, this step requires a distribution η_u over initial states $s \in \beta(u)$.
- Use sampling to estimate the probability $P(e; \pi_e, \eta_u)$ that π_e safely transitions from $\beta(u)$ to $\beta(u')$.
- Use Dijkstra’s algorithm in conjunction with the edge costs $c(e) = -\log(P(e; \pi_e, \eta_u))$ to compute a path $\rho^* = u_0 \rightarrow u_1 \rightarrow \dots \rightarrow u_k$ in \mathcal{G} that minimizes $c(\rho) = -\sum_{j=0}^{k-1} \log(P(e_j; \pi_j, \eta_j))$, where $e_j = u_j \rightarrow u_{j+1}$, $\pi_j = \pi_{e_j}$, and $\eta_j = \eta_{u_j}$.

Algorithm 1 Compositional reinforcement learning algorithm for solving abstract reachability.

```

function DIRL( $\mathcal{M}, \mathcal{G}$ )
  Initialize processed vertices  $U_p \leftarrow \emptyset$ 
  Initialize  $\Gamma_{u_0} \leftarrow \{u_0\}$ , and  $\Gamma_u \leftarrow \emptyset$  for  $u \neq u_0$ 
  Initialize edge policies  $\Pi \leftarrow \emptyset$ 
  while true do
     $u \leftarrow \text{NEARESTVERTEX}(U \setminus U_p, \Gamma, \Pi)$ 
     $\rho_u \leftarrow \text{SHORTESTPATH}(\Gamma_u)$ 
     $\eta_u \leftarrow \text{REACHDISTRIBUTION}(\rho_u, \Pi)$ 
    if  $u \in F$  then return  $\text{PATHPOLICY}(\rho_u, \Pi)$ 
    for  $e = u \rightarrow u' \in \text{Outgoing}(u)$  do
       $\pi_e \leftarrow \text{LEARNPOLICY}(e, \eta_u)$ 
      Add  $\rho_u \circ e$  to  $\Gamma_{u'}$  and  $\pi_e$  to  $\Pi$ 
    Add  $u$  to  $U_p$ 

```

Then, we could choose π to be the sequence of policies π_1, \dots, π_{k-1} —i.e., execute each policy π_j until it reaches $\beta(u_{j+1})$, and then switch to π_{j+1} .

There are two challenges that need to be addressed in realizing this approach effectively. First, it is unclear what distribution to use as the initial state distribution η_u to train π_e . Second, it might be unnecessary to learn all the policies since a subset of the edges might be sufficient for the reachability task. Our algorithm (Algorithm 1) addresses these issues by lazily training π_e —i.e., only training π_e when the edge cost $c(e)$ is needed by Dijkstra’s algorithm.

In more detail, DIRL iteratively processes vertices in \mathcal{G} starting from the initial vertex u_0 , continuing until it processes a final vertex $u \in F$. It maintains the property that for every u it processes, it has already trained policies for all edges along some path ρ_u from u_0 to u . This property is satisfied by u_0 since there is a path of length zero from u_0 to itself. In Algorithm 1, Γ_u is the set of all paths from u_0 to u discovered so far, $\Gamma = \bigcup_u \Gamma_u$, and $\Pi = \{\pi_e \mid e = u \rightarrow u' \in E, u \in U_p\}$ is the set of all edge policies trained so far. In each iteration, DIRL processes an unprocessed vertex u nearest to u_0 , which it discovers using NEARESTVERTEX, and performs the following steps:

1. SHORTESTPATH selects the shortest path from u_0 to u in Γ_u , denoted $\rho_u = u_0 \rightarrow \dots \rightarrow u_k = u$.
2. REACHDISTRIBUTION computes the distribution η_u over states in $\beta(u)$ induced by using the sequence of policies $\pi_{e_0}, \dots, \pi_{e_{k-1}} \in \Pi$, where $e_j = u_j \rightarrow u_{j+1}$ are the edges in ρ_u .
3. For every edge $e = u \rightarrow u'$, LEARNPOLICY learns a policy π_e for e using η_u as the initial state distribution, and adds π_e to Π and $\rho_{u'}$ to $\Gamma_{u'}$, where $\rho_{u'} = u_0 \rightarrow \dots \rightarrow u \rightarrow u'$; π_e is trained to ensure that the resulting trajectories from $\beta(u)$ to $\beta(u')$ are in $\mathcal{Z}_{\text{safe}}^e$ with high probability.

4.2 Definitions and Notation

Edge costs. We begin by defining the edge costs used in Dijkstra’s algorithm. Given a policy π_e for edge $e = u \rightarrow u'$, and an initial state distribution η_u over the subgoal region $\beta(u)$, the cost $c(e)$ of e is the negative log probability that π_e safely transitions the system from $s_0 \sim \eta_u$ to $\beta(u')$. First, we say a trajectory ζ starting at s_0 achieves an e if it safely reaches $\beta(u')$ —formally:

Definition 4.1. An infinite trajectory $\zeta = s_0 \rightarrow s_1 \rightarrow \dots$ achieves edge $e = u \rightarrow u'$ in \mathcal{G} (denoted $\zeta \models e$) if (i) $s_0 \in \beta(u)$, and (ii) there exists i (constrained to be positive if $u \neq u_0$) such that $s_i \in \beta(u')$ and $\zeta_{0:i} \in \mathcal{Z}_{\text{safe}}^e$; we denote the smallest such i by $i(\zeta, e)$.

Then, the probability that π achieves e from an initial state $s_0 \sim \eta_u$ is

$$P(e; \pi_e, \eta_u) = \Pr_{s_0 \sim \eta_u, \zeta \sim \mathcal{D}_{\pi_e, s_0}} [\zeta \models e],$$

where \mathcal{D}_{π_e, s_0} is the distribution over infinite trajectories induced by using π_e from initial state s_0 . Finally, the cost of edge e is $c(e) = -\log P(e; \pi_e, \eta_u)$. Note that $c(e)$ is nonnegative for any edge e .

Path policies. Given edge policies Π along with a path $\rho = u_0 \rightarrow u_1 \rightarrow \dots \rightarrow u_k = u$ in \mathcal{G} , we define a *path policy* π_ρ to navigate from $\beta(u_0)$ to $\beta(u)$. In particular, π_ρ executes $\pi_{u_j \rightarrow u_{j+1}}$ (starting from $j = 0$) until reaching $\beta(u_{j+1})$, after which it increments $j \leftarrow j + 1$ (unless $j = k$). That is, π_ρ

is designed to achieve the sequence of edges in ρ . Note that π_ρ is stateful since it internally keeps track of the index j of the current policy.

Induced distribution. Let path $\rho = u_0 \rightarrow \dots \rightarrow u_k = u$ from u_0 to u be such that edge policies for all edges along the path have been trained. The induced distribution η_ρ is defined inductively on the length of ρ . Formally, for the zero length path $\rho = u_0$ (so $u = u_0$), we define $\eta_\rho = \eta$ to be the initial state distribution of the MDP \mathcal{M} . Otherwise, we have $\rho = \rho' \circ e$, where $e = u' \rightarrow u$. Then, we define η_ρ to be the state distribution over $\beta(u)$ induced by using π_e from $s_0 \sim \eta_{\rho'}$ conditioned on $\zeta \models e$. Formally, η_ρ is the probability distribution over $\beta(u)$ such that for a set of states $S' \subseteq \beta(u)$, the probability of S' according to η_ρ is

$$\Pr_{s \sim \eta_\rho} [s \in S'] = \Pr_{s_0 \sim \eta_{\rho'}, \zeta \sim \mathcal{D}_{\pi_e, s_0}} [s_{i(\zeta, e)} \in S' \mid \zeta \models e].$$

Path costs. The cost of a path $\rho = u_0 \rightarrow \dots \rightarrow u_k = u$ is $c(\rho) = -\sum_{j=0}^{k-1} \log P(e_j; \pi_{e_j}, \eta_{\rho_{0:j}})$ where $e_j = u_j \rightarrow u_{j+1}$ is the j -th edge in ρ , and $\rho_{0:j} = u_0 \rightarrow \dots \rightarrow u_j$ is the j -th prefix of ρ .

4.3 Algorithm Details

DIRL interleaves Dijkstra’s algorithm with using RL to train policies π_e . Note that the edge weights to run Dijkstra’s are not given *a priori* since the edge policies and initial state/induced distributions are unknown. Instead, they are computed on-the-fly beginning from the subgoal region u_0 using Algorithm 1. We describe each subprocedure below.

Processing order (NEARESTVERTEX). On each iteration, DIRL chooses the vertex u to process next to be an unprocessed vertex that has the shortest path from u_0 —i.e., $u \in \arg \min_{u' \in U \setminus U_p} \min_{\rho \in \Gamma_{u'}} c(\rho)$. This choice is an important part of Dijkstra’s algorithm. For a graph with fixed costs, it ensures that the computed path ρ_u to each vertex u is minimized. While the costs in our setting are not fixed since they depend on η_u , this strategy remains an effective heuristic.

Shortest path computation (SHORTESTPATH). This subroutine returns a path of minimum cost, $\rho_u \in \arg \min_{\rho \in \Gamma_u} c(\rho)$. These costs can be estimated using Monte Carlo sampling.

Initial state distribution (REACHDISTRIBUTION). A key choice DIRL makes is what initial state distribution η_u to choose to train policies π_e for outgoing edges $e = u \rightarrow u'$. DIRL chooses the initial state distribution $\eta_u = \eta_{\rho_u}$ to be the distribution of states reached by the path policy π_{ρ_u} from a random initial state $s_0 \sim \eta$.³

Learning an edge policy (LEARNPOLICY). Now that the initial state distribution η_u is known, we describe how DIRL learns a policy π_e for a single edge $e = u \rightarrow u'$. At a high level, it trains π_e using a standard RL algorithm, where the rewards $\mathbb{1}(\zeta \models e)$ are designed to encourage π_e to safely transition the system to a state in $\beta(u')$. To be precise, DIRL uses RL to compute $\pi_e \in \arg \max_\pi P(e; \pi, \eta_u)$. Shaped rewards can be used to improve learning; see Appendix B.

Constructing a path policy (PATHPOLICY). Given edge policies Π along with a path $\rho = u_0 \rightarrow \dots \rightarrow u$, where $u \in F$ is a final vertex, DIRL returns the path policy π_ρ .

Theoretical Guarantee. We have the following guarantee (we give a proof in Appendix C).

Theorem 4.2. *Given a path policy π_ρ corresponding to a path $\rho = u_0 \rightarrow \dots \rightarrow u_k = u$, where $u \in F$, we have $\Pr_{\zeta \sim \mathcal{D}_{\pi_\rho}} [\zeta \models \mathcal{G}] \geq \exp(-c(\rho))$.*

In other words, we guarantee that minimizing the path cost $c(\rho)$ corresponds to maximizing a lower bound on the objective of the abstract reachability problem.

5 Experiments

We empirically evaluate our approach on several continuous control environments; details are in Appendix D, E and F.

³This choice is the distribution of states reaching u by the path policy π_ρ eventually returned by DIRL. Thus, it ensures that the training and test distributions for edge policies in π_ρ are equal.

Rooms environment. We consider the 9-Rooms environment shown in Figure 1, and a similar 16-Rooms environment. They have states $(x, y) \in \mathbb{R}^2$ encoding 2D position, actions $(v, \theta) \in \mathbb{R}^2$ encoding speed and direction, and transitions $s' = s + (v \cos(\theta), v \sin(\theta))$. For 9-Rooms, we consider specifications similar to ϕ_{ex} in Figure 1. For 16-Rooms, we consider a series of increasingly challenging specifications ϕ_1, \dots, ϕ_5 ; each ϕ_i encodes a sequence of i sub-specifications, each of which has the same form as ϕ_{ex} (see Appendix E). We learn policies using ARS [28] with shaped rewards (see Appendix B); each one is a fully connected NN with 2 hidden layers of 30 neurons each.

Fetch environment. We consider the Fetch-Pick-And-Place environment in OpenAI Gym [7], consisting of a robotic arm that can grasp objects and a block to manipulate. The state space is \mathbb{R}^{25} , which includes components encoding the gripper position, the (relative) position of the object, and the distance between the gripper fingers. The action space is \mathbb{R}^4 , where the first 3 components encode the target gripper position and the last encodes the target gripper width. The block’s initial position is a random location on a table. We consider predicates *NearObj* (indicates if the gripper of the arm is close to the block), *HoldingObj* (indicates if the gripper is holding the block), *LiftedObj* (indicates if the block is above the table), and *ObjAt*[g] (indicates if the block is close to a goal $g \in \mathbb{R}^3$).

We consider three specifications. First, *PickAndPlace* is

$$\phi_1 = \text{NearObj}; \text{HoldingObj}; \text{LiftedObj}; \text{ObjAt}[g],$$

where g is a random goal location. Second, *PickAndPlaceStatic* is similar to the previous one, except the goal location is fixed. Third, *PickAndPlaceChoice* involves choosing between two tasks, each of which is a sequence of two subtasks similar to *PickAndPlaceStatic*. We learn policies using TD3 [11] with shaped rewards; each one is a fully connected NN with 2 hidden layers of 256 neurons each.

Baselines. We compare our approach to four state-of-the-art algorithms for learning from specifications, SPECTRL [20], QRM [16], HRM [31], and a TLTL [25] based approach. We used publicly available implementations of SPECTRL, QRM, and HRM. For QRM and HRM, we manually encoded the tasks as reward machines with continuous rewards. The variants QRM+CR and HRM+CR use counterfactual reasoning to reuse samples during training. Our implementation of TLTL uses the quantitative semantics defined in Li et al. [25] with ARS to learn a single policy for each task. Note that DURL returns a policy only after the search finishes. Thus, to plot learning curves, we run our algorithm multiple times with different number of episodes used for learning edge policies.

Results. Figure 3 shows learning curves on the specifications for 16-Rooms environment with all doors open. None of the baselines scale beyond ϕ_2 (one segment), while DURL quickly converges to high-quality policies for all specifications. The TLTL baseline performs poorly since most of these tasks require stateful policies, which it does not support. Though SPECTRL can learn stateful policies, it scales poorly since (i) it does not decompose the learning problem into simpler ones, and (ii) it does not integrate model-based planning at the high-level. Reward Machine based approaches (QRM and HRM) are also unable to handle complex specifications, likely because they are completely based on model-free RL, and do not employ model-based planning at the high-level.

We summarize the scalability in Figure 3f, where we show the average number of steps needed to achieve a given success probability z as a function of the number of edges in \mathcal{G}_ϕ (denoted by $|\mathcal{G}_\phi|$). As can be seen, the sample complexity of DURL scales roughly linearly in the graph size. Intuitively, each subtask takes a constant number of steps to learn, so the total number of steps required is proportional to $|\mathcal{G}_\phi|$. In the supplement, we show learning curves for 9-Rooms (Figure 6) for a variety of specifications, and learning curves for a variant of 16-Rooms with many blocked doors with the same specifications described above (Figure 7). These experiments demonstrate the robustness of our tool on different specifications and environments. For instance, in the 16-Rooms environment with blocked doors, fewer policies satisfy the specification, which makes learning more challenging but DURL is still able to learn high-quality policies for all the specifications.

Next, we show results for the Fetch environment in Figure 4. The trends are similar to before—DURL leverages compositionality to quickly learn effective policies, whereas the baselines are ineffective. The last task is especially challenging, taking DURL somewhat longer to solve, but it ultimately achieves similar effectiveness. These results demonstrate that DURL can scale to complex specifications even in challenging environments with high-dimensional state spaces.

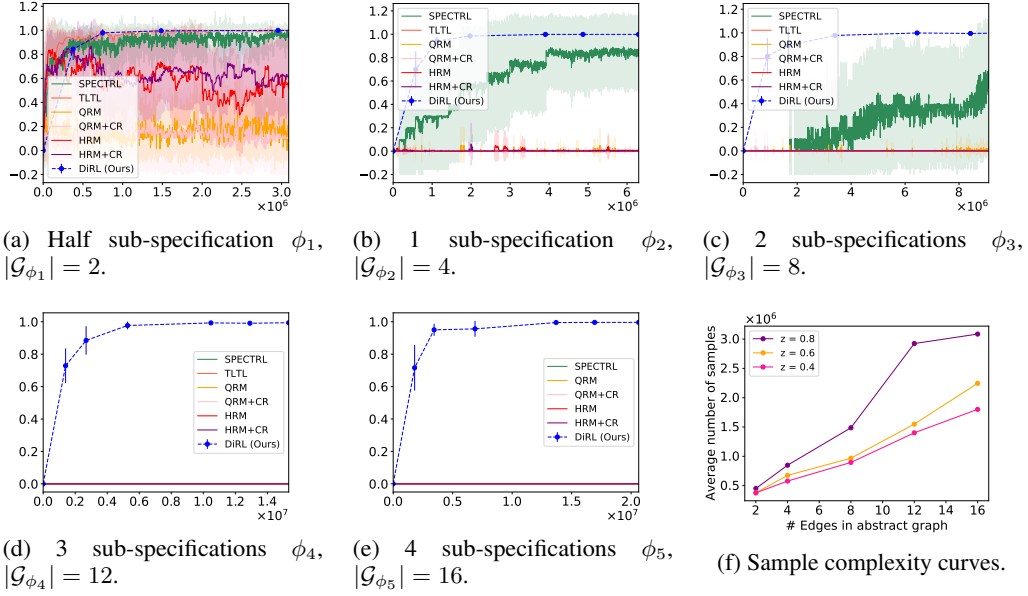


Figure 3: (a)-(e) Learning curves for 16-Rooms environment with different specifications increasing in complexity from (a) to (e). x -axis denotes the number of samples (steps) and y -axis denotes the estimated probability of success. Results are averaged over 10 runs with error bars indicating \pm standard deviation. (f) shows the average number of samples (steps) needed to achieve a success probability $\geq z$ (y -axis) as a function of the size of the abstract graph $|\mathcal{G}_\phi|$.

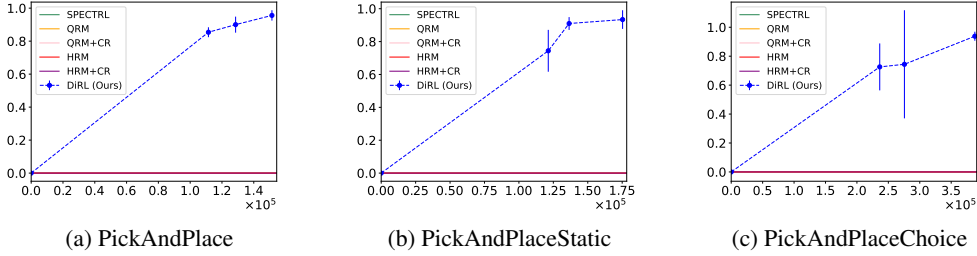


Figure 4: Learning curves for Fetch environment; x -axis denotes the total number of samples (steps) and y -axis denotes the estimated probability of success. Results are averaged over 5 runs with error bars indicating \pm standard deviation.

6 Conclusion

We have proposed DiRL, a reinforcement learning approach for logical specifications that leverages the compositional structure of the specification to decouple high-level planning and low-level control. Our experiments demonstrate that DiRL can effectively solve complex continuous control tasks, significantly improving over existing approaches. Logical specifications are a promising approach to enable users to more effectively specify robotics tasks; by enabling more scalable learning of these specifications, we are directly enabling users to specify more complex objectives through the underlying specification language. While we have focused on SPECTRL specifications, we believe our approach can also enable the incorporation of more sophisticated features into the underlying language, such as conditionals (i.e., only perform a subtask upon observing some property of the environment) and iterations (i.e., repeat a subtask until some objective is met).

Limitations. One limitation of our approach is that we only consider path policies. It is possible that an optimal policy must follow different high-level plans from different states within the same subgoal region. Also, DiRL assumes the ability to sample trajectories starting at any state $s \in S$, whereas in

some cases it might only be possible to obtain trajectories starting at some initial state. We believe these limitations can be addressed in future work by modifying our algorithm appropriately.

References

- [1] David Abel, Nate Umbanhowar, Khimya Khetarpal, Dilip Arumugam, Doina Precup, and Michael Littman. Value preserving state-action abstractions. In *International Conference on Artificial Intelligence and Statistics*, pages 1639–1650. PMLR, 2020.
- [2] Derya Aksaray, Austin Jones, Zhaodan Kong, Mac Schwager, and Calin Belta. Q-learning for robust satisfaction of signal temporal logic specifications. In *Conference on Decision and Control (CDC)*, pages 6565–6570. IEEE, 2016.
- [3] Dario Amodei, Chris Olah, Jacob Steinhardt, Paul Christiano, John Schulman, and Dan Mané. Concrete problems in ai safety. *arXiv preprint arXiv:1606.06565*, 2016.
- [4] Greg Anderson, Abhinav Verma, Isil Dillig, and Swarat Chaudhuri. Neurosymbolic reinforcement learning with formally verified exploration. In *Advances in Neural Information Processing Systems*, 2020.
- [5] Jacob Andreas, Dan Klein, and Sergey Levine. Modular multitask reinforcement learning with policy sketches. In *International Conference on Machine Learning*, pages 166–175, 2017.
- [6] OpenAI: Marcin Andrychowicz, Bowen Baker, Maciek Chociej, Rafal Jozefowicz, Bob McGrew, Jakub Pachocki, Arthur Petron, Matthias Plappert, Glenn Powell, Alex Ray, et al. Learning dexterous in-hand manipulation. *The International Journal of Robotics Research*, 39(1):3–20, 2020.
- [7] Greg Brockman, Vicki Cheung, Ludwig Pettersson, Jonas Schneider, John Schulman, Jie Tang, and Wojciech Zaremba. Openai gym, 2016.
- [8] Alberto Camacho, Rodrigo Toro Icarte, Toryn Q. Klassen, Richard Valenzano, and Sheila A. McIlraith. Ltl and beyond: Formal languages for reward function specification in reinforcement learning. In *International Joint Conference on Artificial Intelligence*, pages 6065–6073, 7 2019.
- [9] Yevgen Chebotar, Karol Hausman, Marvin Zhang, Gaurav Sukhatme, Stefan Schaal, and Sergey Levine. Combining model-based and model-free updates for trajectory-centric reinforcement learning. In *International conference on machine learning*, pages 703–711. PMLR, 2017.
- [10] Steve Collins, Andy Ruina, Russ Tedrake, and Martijn Wisse. Efficient bipedal robots based on passive-dynamic walkers. *Science*, 307(5712):1082–1085, 2005.
- [11] Scott Fujimoto, Herke Hoof, and David Meger. Addressing function approximation error in actor-critic methods. In *International Conference on Machine Learning*, pages 1587–1596, 2018.
- [12] Ernst Moritz Hahn, Mateo Perez, Sven Schewe, Fabio Somenzi, Ashutosh Trivedi, and Dominik Wojtczak. Omega-regular objectives in model-free reinforcement learning. In *Tools and Algorithms for the Construction and Analysis of Systems*, pages 395–412, 2019.
- [13] Lewis Hammond, Alessandro Abate, Julian Gutierrez, and Michael Wooldridge. Multi-agent reinforcement learning with temporal logic specifications. In *International Conference on Autonomous Agents and MultiAgent Systems*, page 583–592, 2021.
- [14] M. Hasanbeig, Y. Kantaros, A. Abate, D. Kroening, G. J. Pappas, and I. Lee. Reinforcement learning for temporal logic control synthesis with probabilistic satisfaction guarantees. In *Conference on Decision and Control (CDC)*, pages 5338–5343, 2019.
- [15] Mohammadhossein Hasanbeig, Alessandro Abate, and Daniel Kroening. Logically-constrained reinforcement learning. *arXiv preprint arXiv:1801.08099*, 2018.
- [16] Rodrigo Toro Icarte, Toryn Klassen, Richard Valenzano, and Sheila McIlraith. Using reward machines for high-level task specification and decomposition in reinforcement learning. In *International Conference on Machine Learning*, pages 2107–2116. PMLR, 2018.

- [17] Jeevana Priya Inala, Osbert Bastani, Zenna Tavares, and Armando Solar-Lezama. Synthesizing programmatic policies that inductively generalize. In *International Conference on Learning Representations*, 2020.
- [18] Jeevana Priya Inala, Yichen Yang, James Paulos, Yewen Pu, Osbert Bastani, Vijay Kumar, Martin Rinard, and Armando Solar-Lezama. Neurosymbolic transformers for multi-agent communication. *arXiv preprint arXiv:2101.03238*, 2021.
- [19] Yuqian Jiang, Sudarshanan Bharadwaj, Bo Wu, Rishi Shah, Ufuk Topcu, and Peter Stone. Temporal-logic-based reward shaping for continuing learning tasks, 2020.
- [20] Kishor Jothimurugan, Rajeev Alur, and Osbert Bastani. A composable specification language for reinforcement learning tasks. In *Advances in Neural Information Processing Systems*, volume 32, pages 13041–13051, 2019.
- [21] Kishor Jothimurugan, Osbert Bastani, and Rajeev Alur. Abstract value iteration for hierarchical reinforcement learning. In *International Conference on Artificial Intelligence and Statistics*, pages 1162–1170. PMLR, 2021.
- [22] Sebastian Junges, Nils Jansen, Christian Dehnert, Ufuk Topcu, and Joost-Pieter Katoen. Safety-constrained reinforcement learning for mdps. In *International Conference on Tools and Algorithms for the Construction and Analysis of Systems*, pages 130–146. Springer, 2016.
- [23] Yen-Ling Kuo, B. Katz, and A. Barbu. Encoding formulas as deep networks: Reinforcement learning for zero-shot execution of ltl formulas. *IEEE/RSJ International Conference on Intelligent Robots and Systems (IROS)*, pages 5604–5610, 2020.
- [24] Sergey Levine, Chelsea Finn, Trevor Darrell, and Pieter Abbeel. End-to-end training of deep visuomotor policies. *The Journal of Machine Learning Research*, 17(1):1334–1373, 2016.
- [25] Xiao Li, Cristian-Ioan Vasile, and Calin Belta. Reinforcement learning with temporal logic rewards. In *IEEE/RSJ International Conference on Intelligent Robots and Systems (IROS)*, pages 3834–3839. IEEE, 2017.
- [26] Michael L. Littman, Ufuk Topcu, Jie Fu, Charles Isbell, Min Wen, and James MacGlashan. Environment-independent task specifications via gltl, 2017.
- [27] Ryan Lowe, Yi Wu, Aviv Tamar, Jean Harb, Pieter Abbeel, and Igor Mordatch. Multi-agent actor-critic for mixed cooperative-competitive environments. *arXiv preprint arXiv:1706.02275*, 2017.
- [28] Horia Mania, Aurelia Guy, and Benjamin Recht. Simple random search of static linear policies is competitive for reinforcement learning. In *Advances in Neural Information Processing Systems*, pages 1805–1814, 2018.
- [29] Cyrus Neary, Zhe Xu, Bo Wu, and Ufuk Topcu. Reward machines for cooperative multi-agent reinforcement learning, 2021.
- [30] Shao-Hua Sun, Te-Lin Wu, and Joseph J. Lim. Program guided agent. In *International Conference on Learning Representations*, 2020.
- [31] Rodrigo Toro Icarte, Toryn Q. Klassen, Richard Valenzano, and Sheila A. McIlraith. Reward machines: Exploiting reward function structure in reinforcement learning. *arXiv preprint arXiv:2010.03950*, 2020.
- [32] Abhinav Verma, Vijayaraghavan Murali, Rishabh Singh, Pushmeet Kohli, and Swarat Chaudhuri. Programmatically interpretable reinforcement learning. In *International Conference on Machine Learning*, pages 5045–5054, 2018.
- [33] Abhinav Verma, Hoang M Le, Yisong Yue, and Swarat Chaudhuri. Imitation-projected programmatic reinforcement learning. In *Advances in Neural Information Processing Systems*, 2019.
- [34] Zhe Xu and Ufuk Topcu. Transfer of temporal logic formulas in reinforcement learning. In *International Joint Conference on Artificial Intelligence*, pages 4010–4018, 7 2019.

- [35] Lim Zun Yuan, Mohammadhosein Hasanbeig, Alessandro Abate, and Daniel Kroening. Modular deep reinforcement learning with temporal logic specifications. *arXiv preprint arXiv:1909.11591*, 2019.

A Reduction to Abstract Reachability

In this section, we detail the construction of the abstract graph \mathcal{G}_ϕ from a SPECTRL specification ϕ . Given two sets of finite trajectories $\mathcal{Z}_1, \mathcal{Z}_2 \subseteq \mathcal{Z}_f$, let us denote by $\mathcal{Z}_1 \circ \mathcal{Z}_2$ the concatenation of the two sets—i.e.,

$$\mathcal{Z}_1 \circ \mathcal{Z}_2 = \left\{ \zeta \in \mathcal{Z}_f \mid \begin{array}{l} \exists i < t. \zeta_{0:i} \in \mathcal{Z}_1 \\ \wedge \zeta_{(i+1):t} \in \mathcal{Z}_2 \end{array} \right\}.$$

In addition to the abstract graph $\mathcal{G} = (U, E, u_0, F, \beta, \mathcal{Z}_{\text{safe}})$ we also construct a set of safe terminal trajectories $\mathcal{Z}_{\text{term}} = \bigcup_{u \in F} \mathcal{Z}_{\text{term}}^u$ where $\mathcal{Z}_{\text{term}}^u \subseteq \mathcal{Z}_f$ is the set of terminal trajectories for the final vertex $u \in F$. Now, we define what it means for a finite trajectory ζ to satisfy the pair $(\mathcal{G}, \mathcal{Z}_{\text{term}})$.

Definition A.1. An finite trajectory $\zeta = s_0 \xrightarrow{a_0} s_1 \xrightarrow{a_1} \dots \xrightarrow{a_{t-1}} s_t$ in \mathcal{M} satisfies the pair $(\mathcal{G}, \mathcal{Z}_{\text{term}})$ (denoted $\zeta \models (\mathcal{G}, \mathcal{Z}_{\text{term}})$) if there is a sequence of indices $0 = i_0 \leq i_1 < \dots < i_k \leq t$ and a path $\rho = u_0 \rightarrow u_1 \rightarrow \dots \rightarrow u_k$ in \mathcal{G} such that

- $u_k \in F$,
- for all $j \in \{0, \dots, k\}$, we have $s_{i_j} \in \beta(u_j)$,
- for all $j < k$, letting $e_j = u_j \rightarrow u_{j+1}$, we have $\zeta_{i_j:i_{j+1}} \in \mathcal{Z}_{\text{safe}}^{e_j}$, and
- $\zeta_{i_k:t} \in \mathcal{Z}_{\text{term}}^{u_k}$.

We now outline the inductive construction of the pair $(\mathcal{G}_\phi, \mathcal{Z}_{\text{term}, \phi})$ from a specification ϕ such that any finite trajectory $\zeta \in \mathcal{Z}_f$ satisfies ϕ if and only if ζ satisfies $(\mathcal{G}_\phi, \mathcal{Z}_{\text{term}, \phi})$.

Objectives ($\phi = \text{achieve } b$). The abstract graph is $\mathcal{G}_\phi = (U, E, u_0, F, \beta, \mathcal{Z}_{\text{safe}})$ where

- $U = \{u_0, u_b\}$ with $\beta(u_0) = S$ and $\beta(u_b) = S_b = \{s \mid s \models b\}$,
- $E = \{u_0 \rightarrow u_b\}$,
- $F = \{u_b\}$ and,
- $\mathcal{Z}_{\text{safe}}^{(u_0, u_b)} = \mathcal{Z}_{\text{term}}^{u_b} = \mathcal{Z}_f$.

Constraints ($\phi = \phi_1$ ensuring b). Let the abstract graph for ϕ_1 be $\mathcal{G}_{\phi_1} = (U_1, E_1, u_0^1, F_1, \beta_1, \mathcal{Z}_{\text{safe}, 1})$ and the terminal trajectories be $\mathcal{Z}_{\text{term}, 1}$. Then, the abstract graph for ϕ is $\mathcal{G}_\phi = (U, E, u_0, F, \beta, \mathcal{Z}_{\text{safe}})$ where

- $U = U_1, u_0 = u_0^1, E = E_1$ and $F = F_1$.
- $\beta(u) = \beta_1(u) \cap S_b$ for all $u \in U \setminus \{u_0\}$ where $S_b = \{s \mid s \models b\}$, and $\beta(u_0) = S$.
- $\mathcal{Z}_{\text{safe}}^e = \mathcal{Z}_{\text{safe}, 1}^e \cap \mathcal{Z}_b$ for all $e \in E$ where

$$\mathcal{Z}_b = \{\zeta \in \mathcal{Z}_f \mid \forall i. s_i \models b\}.$$

- $\mathcal{Z}_{\text{term}}^u = \mathcal{Z}_{\text{term}, 1}^u \cap \mathcal{Z}_b$ for all $u \in F$.

Sequencing ($\phi = \phi_1; \phi_2$). Let the abstract graph for ϕ_i be $\mathcal{G}_{\phi_i} = (U_i, E_i, u_0^i, F_i, \beta_i, \mathcal{Z}_{\text{safe}, i})$ and the terminal trajectories be $\mathcal{Z}_{\text{term}, i}$ for $i \in \{1, 2\}$. The abstract graph $\mathcal{G}_\phi = (U, E, u_0, F, \beta, \mathcal{Z}_{\text{safe}})$ is constructed as follows.

- $U = U_1 \sqcup U_2 \setminus \{u_0^2\}$.
- $E = E_1 \sqcup E_2' \sqcup E_{1 \rightarrow 2}$ where

$$E_2' = \{u \rightarrow u' \in E_2 \mid u \neq u_0^2\} \quad \text{and}$$

$$E_{1 \rightarrow 2} = \{u^1 \rightarrow u^2 \mid u^1 \in F_1 \ \& \ u_0^2 \rightarrow u^2 \in E_2\}.$$

- $u_0 = u_0^1$ and $F = F_2$.
- $\beta(u) = \beta_i(u)$ for all $u \in U_i$ and $i \in \{1, 2\}$.
- The safe trajectories are given by

- $\mathcal{Z}_{\text{safe}}^e = \mathcal{Z}_{\text{safe},1}^e$ for all $e \in E_1$,
- $\mathcal{Z}_{\text{safe}}^e = \mathcal{Z}_{\text{safe},2}^e$ for all $e \in E_2'$ and,
- $\mathcal{Z}_{\text{safe}}^{u^1 \rightarrow u^2} = \mathcal{Z}_{\text{term},1}^{u^1} \circ \mathcal{Z}_{\text{safe},2}^{u_0^2 \rightarrow u^2}$ for all $u^1 \rightarrow u^2 \in E_{1 \rightarrow 2}$.
- $\mathcal{Z}_{\text{term}}^u = \mathcal{Z}_{\text{term},2}^u$ for all $u \in F$.

Choice ($\phi = \phi_1$ or ϕ_2). Let the abstract graph for ϕ_i be $\mathcal{G}_{\phi_i} = (U_i, E_i, u_0^i, F_i, \beta_i, \mathcal{Z}_{\text{safe},i})$ and the terminal trajectories be $\mathcal{Z}_{\text{term},i}$ for $i \in \{1, 2\}$. The abstract graph for ϕ is $\mathcal{G}_\phi = (U, E, u_0, F, \beta, \mathcal{Z}_{\text{safe}})$ where:

- $U = (U_1 \setminus \{u_0^1\}) \sqcup (U_2 \setminus \{u_0^2\}) \sqcup \{u_0\}$.
- $E = E_1' \sqcup E_2' \sqcup E_0$ where

$$E_i' = \{u \rightarrow u' \in E_i \mid u \neq u_0^i\} \quad \text{and}$$

$$E_0 = \{u_0 \rightarrow u^i \mid i \in \{1, 2\} \ \& \ u_0^i \rightarrow u^i \in E_i\}.$$
- $F = F_1 \sqcup F_2$.
- $\beta(u) = \beta_i(u)$ for all $u \in U_i, i \in \{1, 2\}$ and $\beta(u_0) = S$.
- The safe trajectories are given by
 - $\mathcal{Z}_{\text{safe}}^e = \mathcal{Z}_{\text{safe},i}^e$ for all $e \in E_i'$ and $i \in \{1, 2\}$,
 - $\mathcal{Z}_{\text{safe}}^{u_0 \rightarrow u^i} = \mathcal{Z}_{\text{safe},i}^{u_0^i \rightarrow u^i}$ for all $u_0 \rightarrow u^i \in E_0$ with $u^i \in U_i$.
- $\mathcal{Z}_{\text{term}}^u = \mathcal{Z}_{\text{term},i}^u$ for all $u \in F_i$ and $i \in \{1, 2\}$.

The constructed pair $(\mathcal{G}_\phi, \mathcal{Z}_{\text{term},\phi})$ has the following important properties.

Lemma A.2. *For any SPECTRL specification ϕ , the following hold.*

- For any finite trajectory $\zeta \in \mathcal{Z}_f, \zeta \models \phi$ if and only if $\zeta \models (\mathcal{G}_\phi, \mathcal{Z}_{\text{term},\phi})$.
- For any final vertex u of \mathcal{G}_ϕ and any state $s \in \beta(u)$, the length-1 trajectory $\zeta = s$ is contained in $\mathcal{Z}_{\text{term},\phi}^u$.

Proof. Follows from the above construction by structural induction on ϕ . □

Proof of Theorem 3.4. Let $\zeta = s_0 \xrightarrow{a_0} s_1 \xrightarrow{a_1} \dots$ be an infinite trajectory. First we show that $\zeta \models \phi$ if and only if $\zeta \models \mathcal{G}_\phi$.

(\implies) Suppose $\zeta \models \phi$. Then, there is a $t \geq 0$ such that $\zeta_{0:t} \models \phi$. From Lemma A.2, we get that $\zeta_{0:t} \models (\mathcal{G}_\phi, \mathcal{Z}_{\text{term},\phi})$ which implies that $\zeta \models \mathcal{G}_\phi$.

(\impliedby) Suppose $\zeta \models \mathcal{G}_\phi$. Then, let $0 = i_0 \leq i_1 < \dots < i_k$ be a sequence of indices realizing a path $u_0 \rightarrow \dots \rightarrow u_k$ to a final vertex u_k in \mathcal{G}_ϕ . Since $s_{i_k} \in \beta(u_k)$, from Lemma A.2 we have $\zeta_{i_k:i_k} \in \mathcal{Z}_{\text{term},\phi}^{u_k}$ and hence $\zeta_{0:i_k} \models (\mathcal{G}_\phi, \mathcal{Z}_{\text{term},\phi})$. From Lemma A.2 we conclude that $\zeta_{0:i_k} \models \phi$ and therefore $\zeta \models \phi$.

Next, it follows by a straightforward induction on ϕ that the number of vertices in \mathcal{G}_ϕ is at most $|\phi| + 1$ where $|\phi|$ is the number of operators (achieve, ensuring, ;, or) in ϕ . □

B Shaped Rewards for Learning Policies

To improve learning, we use shaped rewards for learning each edge policy π_e . To enable reward shaping, we assume that the atomic predicates additionally have a *quantitative semantics*—i.e., each atomic predicate $p \in \mathcal{P}_0$ is associated with a function $\llbracket p \rrbracket_q : S \rightarrow \mathbb{R}$. To ensure compatibility with the Boolean semantics, we assume that

$$\llbracket p \rrbracket(s) = (\llbracket p \rrbracket_q(s) > 0). \quad (1)$$

For example, given a state $s \in S$, the atomic predicate

$$\llbracket \text{reach } s \rrbracket_q(s') = 1 - \|s' - s\|$$

indicates whether the system is in a state near s w.r.t. some norm $\|\cdot\|$. In addition, we can extend the quantitative semantics to predicates $b \in \mathcal{P}$ by recursively defining $\llbracket b_1 \wedge b_2 \rrbracket_q(s) = \min\{\llbracket b_1 \rrbracket_q(s), \llbracket b_2 \rrbracket_q(s)\}$ and $\llbracket b_1 \vee b_2 \rrbracket_q(s) = \max\{\llbracket b_1 \rrbracket_q(s), \llbracket b_2 \rrbracket_q(s)\}$. These definitions are a standard extension of Boolean logic to real values. In particular, they preserve (1)—i.e., $b \models s$ if and only if $\llbracket b \rrbracket_q(s) > 0$.

In addition to quantitative semantics, we make use of the following property to define shaped rewards.

Lemma B.1. *The abstract graph $\mathcal{G}_\phi = (U, E, u_0, F, \beta, \mathcal{Z}_{\text{safe}})$ of a specification ϕ satisfies the following:*

- For every non-initial vertex $u \in U \setminus \{u_0\}$, there is a predicate $b \in \mathcal{P}$ such that $\beta(u) = S_b = \{s \mid s \models b\}$.
- For every $e \in E$, either $\mathcal{Z}_{\text{safe}}^e = \mathcal{Z}_b = \{\zeta \in \mathcal{Z} \mid \forall i. s_i \models b\}$ for some $b \in \mathcal{P}$ or $\mathcal{Z}_{\text{safe}}^e = \mathcal{Z}_{b_1} \circ \mathcal{Z}_{b_2}$ for some $b_1, b_2 \in \mathcal{P}$.

Proof sketch. We prove a stronger property that, in addition to the above, requires that for any $e = u_0 \rightarrow u \in E$, $\mathcal{Z}_{\text{safe}}^e = \mathcal{Z}_b$ for some $b \in \mathcal{P}$ and for any final vertex u , $\mathcal{Z}_{\text{term}, \phi}^u = \mathcal{Z}_b$ for some $b \in \mathcal{P}$. This stronger property follows from a straightforward induction on ϕ . \square

Next, we describe the shaped rewards we use to learn an edge $e = u \rightarrow u'$ in \mathcal{G}_ϕ , which have the form

$$R_{\text{step}}(s, a, s') = R_{\text{reach}}(s, a, s') + R_{\text{safe}}(s, a, s').$$

Intuitively, the first term encodes a reward for reaching $\beta(u')$, and the second term encodes a reward for maintaining safety. By Lemma B.1, $\beta(u') = S_b$ for some $b \in \mathcal{P}$. Then, we define

$$R_{\text{reach}}(s, a, s') = \llbracket b \rrbracket_q(s').$$

The safety reward is defined by

$$R_{\text{safe}}(s, a, s') = \begin{cases} \min\{0, \llbracket b \rrbracket_q(s')\} & \text{if } \mathcal{Z}_{\text{safe}}^e = \mathcal{Z}_b \\ \min\{0, \llbracket b \vee b' \rrbracket_q(s')\} & \text{if } \mathcal{Z}_{\text{safe}}^e = \mathcal{Z}_b \circ \mathcal{Z}_{b'} \wedge \psi_b \\ \min\{0, \llbracket b' \rrbracket_q(s')\} & \text{if } \mathcal{Z}_{\text{safe}}^e = \mathcal{Z}_b \circ \mathcal{Z}_{b'} \wedge \neg\psi_b. \end{cases}$$

Here, ψ_b is internal state keeping track of whether b has held so far—i.e., $\psi_b \leftarrow \psi_b \wedge \llbracket b \rrbracket(s)$ at state s . Intuitively, the first case is the simpler case, which checks if every state in the trajectory satisfies b , and the latter two cases handle a sequence where b should hold for the first part of the trajectory, and b' should hold for the remainder.

C Proof of Theorem 4.2

Proof. Let the abstract graph be $\mathcal{G} = (U, E, u_0, F, \beta, \mathcal{Z}_{\text{safe}})$. Let us first define what it means for a rollout to achieve a path in \mathcal{G} .

Definition C.1. *We say that an infinite trajectory ζ achieves the path ρ (denoted $\zeta \models \rho$) if $\zeta \models \mathcal{G}_\rho$ where $\mathcal{G}_\rho = (U_\rho, E_\rho, u_0, \{u\}, \beta \downarrow \rho, \mathcal{Z}_{\text{safe}} \downarrow_\rho)$ with $U_\rho = \{u_j \mid 0 \leq j \leq k\}$, $E_\rho = \{u_j \rightarrow u_{j+1} \mid 0 \leq j < k\}$ and $\beta \downarrow \rho$ and $\mathcal{Z}_{\text{safe}} \downarrow_\rho$ are β and $\mathcal{Z}_{\text{safe}}$ restricted to the vertices and the edges of \mathcal{G}_ρ , respectively.*

From the definition it is clear that for any infinite trajectory ζ , if $\zeta \models \rho$ then $\zeta \models \mathcal{G}$ and therefore

$$\Pr_{\zeta \sim \mathcal{D}_{\pi_\rho}} [\zeta \models \mathcal{G}] \geq \Pr_{\zeta \sim \mathcal{D}_{\pi_\rho}} [\zeta \models \rho]. \quad (2)$$

Let us now define a slightly stronger notion of achieving an edge.

Definition C.2. An infinite trajectory $\zeta = s_0 \rightarrow s_1 \rightarrow \dots$ is said to greedily achieve the path ρ (denoted $\zeta \models_g \rho$) if there is a sequence of indices $0 = i_0 \leq i_1 < \dots < i_k$ such that for all $j < k$,

- $\zeta_{i_j:\infty} \models e_j = u_j \rightarrow u_{j+1}$ and,
- $i_{j+1} = i(\zeta_{i_j:\infty}, e_j)$,

where $\zeta_{i_j:\infty} = s_{i_j} \rightarrow s_{i_j+1} \rightarrow \dots$.

That is, $\zeta \models_g \rho$ if a partition of ζ realizing ρ can be constructed greedily by picking i_{j+1} to be the smallest index $i \geq i_j$ (strictly bigger if $j > 0$) such that $s_i \in \beta(u_{j+1})$ and $\zeta_{i_j:i} \in \mathcal{Z}_{\text{safe}}^{e_j}$. Since $\zeta \models_g \rho$ implies $\zeta \models \rho$, we have

$$\Pr_{\zeta \sim \mathcal{D}_{\pi_\rho}} [\zeta \models \rho] \geq \Pr_{\zeta \sim \mathcal{D}_{\pi_\rho}} [\zeta \models_g \rho]. \quad (3)$$

Let $\rho_{j:k}$ denote the j -th suffix of ρ . We can decompose the probability $\Pr_{\zeta \sim \mathcal{D}_{\pi_\rho}} [\zeta \models_g \rho]$ as follows.

$$\begin{aligned} \Pr_{\zeta \sim \mathcal{D}_{\pi_\rho}} [\zeta \models_g \rho] &= \Pr_{\zeta \sim \mathcal{D}_{\pi_\rho}} [\zeta \models e_0 \wedge \zeta_{i(\zeta, e_0):\infty} \models_g \rho_{1:k}] \\ &= \Pr_{\zeta \sim \mathcal{D}_{\pi_{e_0}}} [\zeta \models e_0] \cdot \Pr_{\zeta \sim \mathcal{D}_{\pi_\rho}} [\zeta_{i(\zeta, e_0):\infty} \models_g \rho_{1:k} \mid \zeta \models e_0] \\ &= P(e_0; \pi_{e_0}, \eta_0) \cdot \Pr_{s_0 \sim \eta_{\rho_{0:1}}, \zeta \sim \mathcal{D}_{\pi_{\rho_{1:k}}, s_0}} [\zeta \models_g \rho_{1:k}] \end{aligned}$$

where the last equality followed from the definition of $\eta_{\rho_{0:1}}$ and the Markov property of \mathcal{M} . Applying the above decomposition recursively, we get

$$\begin{aligned} \Pr_{\zeta \sim \mathcal{D}_{\pi_\rho}} [\zeta \models_g \rho] &= \prod_{j=0}^{k-1} P(e_j; \pi_{e_j}, \eta_{\rho_{0:j}}) \\ &= \exp(\log(\prod_{j=0}^{k-1} P(e_j; \pi_{e_j}, \eta_{\rho_{0:j}}))) \\ &= \exp(-(-\sum_{j=0}^{k-1} \log P(e_j; \pi_{e_j}, \eta_{\rho_{0:j}}))) \\ &= \exp(-c(\rho)). \end{aligned}$$

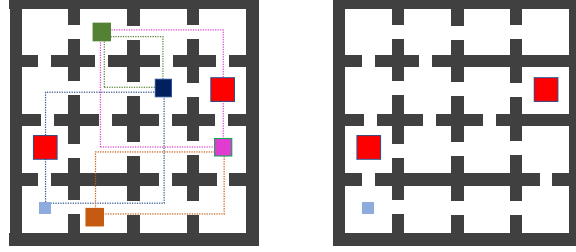
Therefore, from Equations 2 and 3, we get the required bound. \square

D Experimental Methodology

Our tool learns the low-level NN policies for edges using an off-the-shelf RL algorithm. For the Rooms and Fetch environments, we learn policies using ARS [28] and TD3 [11] with shaped rewards, respectively.

For each specification on an environment, we first construct its abstract graph. In DiRL, each edge policy π_e is trained using k episodes of interactions with the environment. For the purpose of generating a learning curve, we run DiRL for each specification with several values of k . For each k value, we plot the sum total of the samples taken to train all edge policies against the probability with which the computed policy reaches a final subgoal region.

For a fair comparison with the baselines, if each episode for learning an edge policy in DiRL is run for m steps, we run the episodes of the baselines for $m \cdot d + c$ steps, where d is the maximum path length to reach a final vertex in the abstract graph of the specification and $c > 0$ is a buffer. Intuitively, this approach ensures that all tools get a similar number of steps in each episode to learn the specification.



(a) 16-Rooms (All doors open) (b) 16-Rooms (Some doors open)

Figure 5: 16-Rooms Environments. Blue square indicates the initial room. Red squares represent obstacles. (a) illustrates the segments in the specifications.

E Case Study: Rooms Environment

We consider environments with several interconnected rooms. The rooms are separated by thick walls and are connected through bi-directional doors.

The environments are a 9-Rooms environment, (Figure 1), a 16-Rooms environment with all doors open (Figure 5a), and 16-Rooms environment with some doors open (Figure 5b). The red blocks indicate obstacles. A robot can pass through those rooms by moving around the red blocks. The robot is initially placed randomly in the center of the room with the blue box (bottom-left corner).

Rooms are identified by the tuple (r, c) denoting the room in the r -th row and c -th column. We use the convention that the bottom-left corner is room $(0,0)$. Predicate $\text{reach}(r, c)$ is interpreted as reaching the center of the (r, c) -th room and predicate $\text{avoid}(r, c)$ is interpreted as avoiding the center of the (r, c) -th room. For clarity, we omit the word *achieve* from specifications of the form *achieve b* denoting such a specification using just the predicate b .

E.1 9-Rooms Environment

Specifications.

1. $\phi_1 := \text{reach}(2, 0); \text{reach}(0, 0)$
Go to the top-left corner and then return to the bottom-left corner (initial room); red blocks not considered obstacles.
This specification is difficult for standard RL algorithms that do not store whether the first sub-task has been achieved. In these cases, a stateless policy will not be able to determine whether to move upwards or downwards. In contrast, D1RL (as well as SPECTRL and RM based approaches) augment the state space to automatically keep track of which sub-tasks have been achieved so far.
2. $\phi_2 := \text{reach}(2, 0) \text{ or } \text{reach}(0, 2)$
Either go to the top-left corner or to the bottom-right corner (obstacles are not considered).
3. $\phi_3 := \phi_2; \text{reach}(2, 2)$
After completing ϕ_2 , go to the top-right corner (obstacles not considered).
This specification combines two choices of similar difficulty yet only one is favorable to fulfilling the specification since the direct path to the top-right corner from the bottom-right one is obstructed by walls.
4. $\phi_4 := \text{reach}(2, 0) \text{ ensuring } \text{avoid}(1, 0)$
Reach the top-left (while considering the obstacles).
5. $\phi_5 := \phi_4 \text{ or } \text{reach}(0, 2); \text{reach}(2, 2)$
Either go to the top-left corner or bottom-right corner enroute to the top-right corner (while considering the obstacles).
This specification is similar to ϕ_3 except that the choices are of unequal difficulty due to the placement of the red obstacle. In this case, the non-greedy choice is favorable for completing the task.

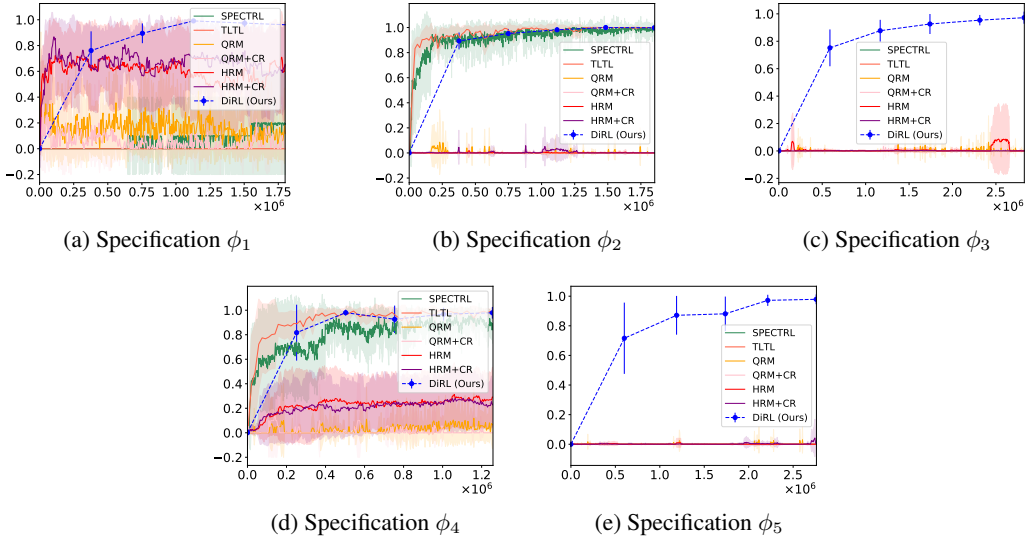


Figure 6: Learning curves for 9-Rooms environment with different specifications. x -axis denotes the number of samples (steps) and y -axis denotes the estimated probability of success. Results are averaged over 10 runs with error bars indicating \pm standard deviation.

Hyperparameters. The edge policies are learned using ARS [28] (version V2-t) with neural network policies and the following hyperparameters.

- Step-size $\alpha = 0.3$.
- Standard deviation of exploration noise $\nu = 0.05$.
- Number of directions sampled per iteration is 30.
- Number of top performing directions to use $b = 15$.

To plot the learning curve, we use values of

$$k \in \{3000, 6000, 12000, 18000, 24000, 30000\}$$

where each episode consists of $m = 20$ steps.

Results. The learning curves for these specifications are shown in Figure 6. While most tools perform reasonably well on specifications ϕ_2 (Figure 6b) and ϕ_4 (Figure 6d), the baselines are unable to learn to satisfy ϕ_3 (Figure 6c) and ϕ_5 (Figure 6e).

E.2 16-Rooms Environment

Specifications. We describe the five specifications used for the 16-rooms environment, which are designed to increase in difficulty. First, we define a *segment* as the following specification: Given the current location of the agent, the goal is to reach a room diagonally opposite to it by visiting at least one of the rooms at the remaining two corners of the rectangle formed by the current room and the goal room—e.g., in the 9-Rooms environment, to visit S_3 from the initial room, the agent must visit either S_1 or S_2 first.

Then, we design specifications of varying sizes by sequencing several segments one after the other. In the first segment, the agent’s current location is the initial room. In subsequent segments, the current location is the goal room of the previous segment. In addition, the agent must always avoid the obstacles in the environment. We create five such specifications, one half-segment and specifications up to four segments (ϕ_1 to ϕ_5), as illustrated in Figure 5a and described below:

1. ϕ_1 corresponds to the *half-segment* enroute (2,2) from (0,0). Thus ϕ_1 is a choice between (0,2) and (2,0).
2. ϕ_2 is the first segment that goes from (0,0) to (2,2)

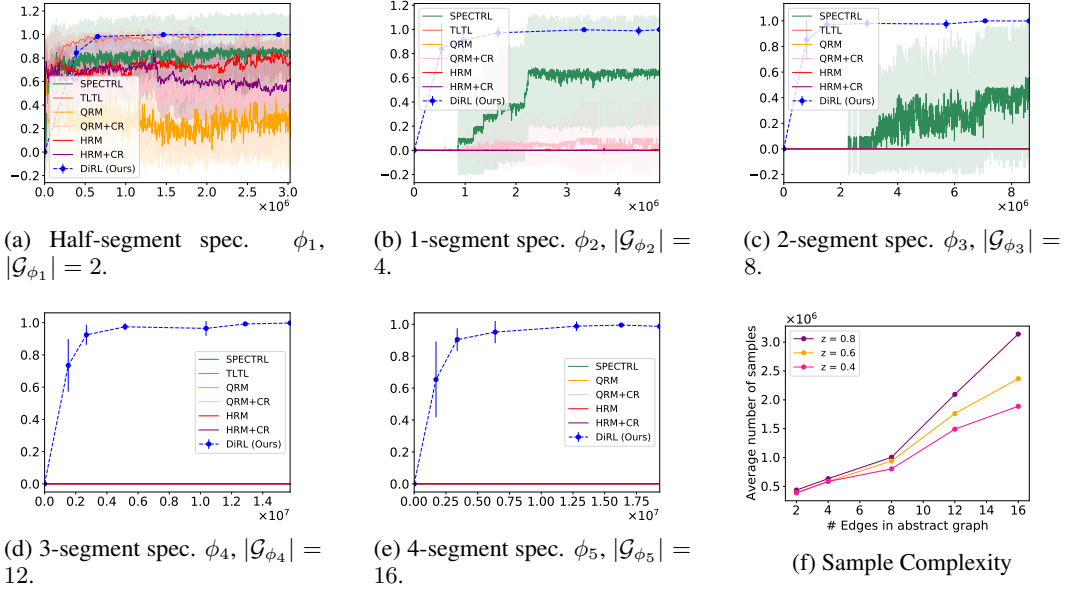


Figure 7: (a)-(e) Learning curves for 16-Rooms environment with some blocked doors (Figure 5b) with different specifications increasing in complexity from (a) to (e). x -axis denotes the number of samples (steps) and y -axis denotes the estimated probability of success. Results are averaged over 10 runs with error bars indicating \pm standard deviation. (f) shows the average number of samples (steps) needed to achieve a success probability $\geq z$ (y -axis) as a function of the size of the abstract graph $|\mathcal{G}_\phi|$.

3. ϕ_3 augments ϕ_2 with a second segment to (3,1).
4. ϕ_4 augments ϕ_3 with a segment to (1,3)
5. ϕ_5 augments ϕ_4 with a segment to (0,1)

We denote by $|\mathcal{G}_\phi|$ the number of edges in the abstract graph corresponding to the specification ϕ .

Hyperparameters. We use the same hyperparameters of ARS as the ones used for the 9-Rooms environment. We run experiments for

$$k \in \{6000, 12000, 24000, 48000, 60000, 72000\}.$$

Results. The learning curves for the environment with all open doors and the constrained environment with some open doors are shown in Figure 3 and Figure 7, respectively.

F Case Study: Fetch Environment

The fetch robotic arm from OpenAI Gym is visualized in Figure 8. Let us denote by $s_r = (s_r^x, s_r^y, s_r^z) \in \mathbb{R}^3$ the position of the gripper, $s_o \in \mathbb{R}^3$ the relative position of the object (black block) w.r.t. the gripper, $s_g \in \mathbb{R}^3$ the goal location (red sphere) and $s_w \in \mathbb{R}$ the width of the gripper. Let c denote the width of the object and $z_\epsilon = (0, 0, \epsilon + c)$ for $\epsilon > 0$. Then, we define the following predicates.

- *NearObj* holds true in states in which the gripper is wide open, aligned with the object and is slightly above the object:

$$\text{NearObj}(s) = (\|s_o + z_\epsilon\|_2^2 + (s_w - 2c)^2 < \delta_1)$$

- *HoldingObj* holds true in states in which the gripper is close to the object and its width is close to the object's width:

$$\text{HoldingObj}(s) = (\|s_o\|_2^2 + (s_w - c)^2 < \delta_2)$$

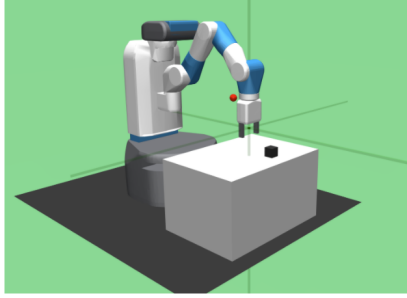


Figure 8: Fetch robotic arm.

- *LiftedObj* holds true in states in which the object is above the surface level of the table:

$$\text{LiftedObj}(s) = (s_r^z + s_o^z > \delta_3)$$

- *ObjAt*[g] holds true in states in which the object is close to g :

$$\text{ObjAt}[g](s) = (\|s_r + s_o - g\|_2^2 < \delta_4)$$

Then the specifications we use are the following.⁴

- *PickAndPlace*: $\phi_1 = \text{NearObj}; \text{HoldingObj}; \text{LiftedObj}; \text{ObjAt}[s_g]$.
- *PickAndPlaceStatic*: $\text{NearObj}; \text{HoldingObj}; \text{LiftedObj}; \text{ObjAt}[g_1]$ where g_1 is a fixed goal.
- *PickAndPlaceChoice*: $(\text{NearObj}; \text{HoldingObj}; \text{LiftedObj}); ((\text{ObjAt}[g_1]; \text{ObjAt}[g_2]) \text{ or } (\text{ObjAt}[g_3]; \text{ObjAt}[g_4]))$.

Hyperparameters. We use TD3 [11] for learning edge policies with the following hyperparameters.

- Discount $\gamma = 0.95$.
- Adam optimizer; actor learning rate 0.0001; critic learning rate 0.001.
- Soft update targets $\tau = 0.005$.
- Replay buffer of size 200000.
- 100 training steps performed every 100 environment steps.
- A minibatch of 256 steps used per training step.
- Exploration using gaussian noise with $\sigma = 0.15$.

We run experiments for $k \in \{1000, 2000, 4000\}$ and each episode consists of $m = 40$ steps.

⁴We denote `achieve b` using just the predicate b .